Novel semiconducting iron-quinizarin metal-organic framework for application in supercapacitors

Surabhi Agrawal[1,2], Stuart M. Clarke[1,2*], Inigo J. Vitorica-Yrezabal[3], Cheng Liu[4], Wei Fang [1], Paul T. Wood[1] and Dominic Wright[1],

[1]Department of Chemistry, University of Cambridge, Cambridge CB2 1EW, UK
[2]BP Institute, University of Cambridge, Cambridge CB3 0EZ, UK
[3]School of Chemistry, University of Manchester, Manchester M13 9PL, UK
[4]Cavendish Laboratory, University of Cambridge, Cambridge CB3 0HE, UK

*address correspondence to this author

Dedication to Prof Alan Soper FRS

We are pleased to submit this article for the special edition to mark the retirement of Prof. Alan Soper. Alan was a central figure in our previous work addressing the structure of supercapacitor ionic solutions and hence it is appropriate for this work that considers novel materials for supercapacitor electrodes. Alan has been a very significant figure in our scientific world, particularly through his development of total scattering to address the structural solution of complex fluids. There can be no doubt that this dynamic and active area of science owes a great deal to Alan's pioneering work and particularly his work to make data analysis accessible for a wide range of users. We, like many others, came to this area through Alan's enormous scientific input. However, in addition, and possibly more importantly, he is the most pleasant and best of men - unfailingly charming and helpful, to even the most troublesome of users.

Abstract

We present conductivity data for a newly synthesised metal organic framework FeQ, $Fe(C_{14}H_6O_4).H_2O$ demonstrating significant electronic transport. The electrical conductivity of the material is expected to be through the π-π interaction of the ligand- quinizarin and is measured to be 1.73×10^{-2} Scm^{-1}. Its potential role as supercapacitor electrodes is discussed.

Keywords: metal-organic framework, semiconducting, supercapacitor, MOF, porous channels

1. Introduction

1.1 Introduction to supercapacitors

With the drive to store intermittent energy from renewable sources (e.g. wind and solar) supercapacitors have become a subject of great interest. These devices function by the formation of aligned ionic layers (capacitive 'double layers') at the surface of electrodes on application of an electric field. This does not require any chemical reaction and hence can have a much faster response than a battery (hence high power and faster charging rate) and is less prone to degradation on cycling.[1,2]

1.2 Characteristics of Supercapacitor Electrodes

To obtain a very high charge storage capacity, high surface area materials are required. The ionic double layers are formed of electrolyte ions and polarised solvent molecules adsorbed onto a substrate making high surface area a requirement for the electrode. Typical substrate materials include graphene/graphene materials with specific surface area ranging between 350-920 m^2g^{-1}.[3-5]

These supercapacitor substrates ideally need to be conducting; hence it is not uncommon to use graphitic materials. However, the substrates usually employed are powdered and need to be held together by a binder, often a polymer (e.g. PVDF, which is insulating), and placed against a metal plate current collector. It would be expected to be an improvement if the material could be conducting and self-supporting. Additionally, if there is a chemical bond to the current collector, then one may expect better conduction than from physical contact alone.

The porous nature of the electrode is also believed to be significant. An optimum has been reported where the size of the pores is just large enough for the unsolvated ion to be admitted, but not the solvated ion.[6] Hence, an electrode with well-defined and controllable pore size is desirable.

1.3 Metal organic frameworks (MOFs) as candidates

In meeting these demands MOFs could be ideal - they have a framework structure for transport of other species. They have well-defined and controllable pore sizes and because the species can enter the entire material (not just an exposed surface) the capacity should be enormous.[7] However, to be completely effective, they should ideally be conducting. Hence, in this work we aim to prepare and characterise a MOF that has significant conductivity. A few examples of supercapacitors with conductive MOF electrodes are known but these are pressed pellets, either standalone or mixed with a conductive binder.[8-11] In the ideal case, the MOF will be prepared on some suitable substrate to ensure optimum current collection, and without the need for polymer binders.

Previous materials

There have been several MOFs that have been reported with some significant conduction capabilities. These are listed below in table 1. However, in most cases the conduction is relatively modest. Details of how these materials conduct is not clear. In conducting coordination compounds of transition metals, it is expected that the localised d orbital of the metal interacts with the electron rich organic network resulting in π-d electron exchange for conduction.[12] One interpretation is that inter ligand interactions via π-π conduction are more significant than conductivity from ligand-to-metal-to-ligand due to inefficient connection between the inorganic and organic units.[7]

In the metal-organic framework $Ni_3(HITP)_2$ (HITP-2,3,6,7,10,11-hexaiminotriphenylene), anisotropic conduction is proposed to occur through the π-π stacks of triphenylene rings of the organic linker.[13] Interestingly for $Cu[Ni(PDT)_2]$, *Kobayashi et al.*[14] suggest that conduction occurs through the redox active nickel bis-dithiolate and copper pyrazine units of the framework. A few metal-organic frameworks have been treated with redox-active conjugated molecules such as 7,7,8,8-tetracyanoquinododimethane, which when trapped in the pores of the framework, are reported to induce electrical conductivity.[15]

Hence, inspired by recent work, here we aim to synthesise conductive metal-organic frameworks using a non-traditional aromatic ligand which has not been used as a linker before.

Table 1: Conducting metal-organic framework materials reported in literature (arranged in order of decreasing electrical conductivity)

Metal-Organic Framework	Metal Center	Organic Linker	Conductivity (S cm^{-1}), Measurement method	Specific Surface Area (m^2g^{-1})	Pore size (nm)	Reference
CuHT	Cu^{2+}	HT- 4-hydroxythiophenol 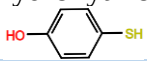	120 pellet- 4 point method	not reported	not reported	[16]
$Cu_3(HIB)_2$	Cu^{2+}	HIB- imine form of hexaaminobenzene 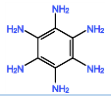	13 pellet- 4 point method	114	not reported	[17]
$Ni_3(HIB)_2$	Ni^{2+}	HIB- imine form of hexaaminobenzene	8 pellet- 4 point method	152	not reported	[17]
$Ni_3(HITP)_2$	Ni^{2+}	HITP- 2,3,6,7,10,11-hexaiminotriphenylene 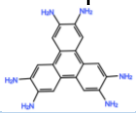	2 pellet- 2 point method	630	1.5	[13]
$Cu_3(HITP)_2$	Cu^{2+}	HITP- 2,3,6,7,10,11-hexaiminotriphenylene	2×10^{-1} pellet- 2 point method	not reported	not reported	[18]
NiPc-MOF	Ni^{2+}	Pc- phthalocyanine 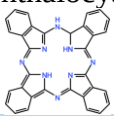	2×10^{-1} Thin film deposited on glass	593	not reported	[19]
$(NBu_4)_2Fe_2(DHBQ)_3$ *(NBu- tetrabutyl ammonium ion)*	Fe^{3+}	DHBQ- 2,5-dioxidobenzoquinone 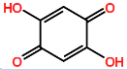	1.6×10^{-1} pellet- 2 point method	No microporosity	N.A.	[20]
$Ni_3(BHT)$	Ni^{2+}	BHT- Benzenehexathiol 	1.5×10^{-1} pellet- 2 point method	not reported	not reported	[21]

NiIT	Ni^{2+}	IT- imine form of 1,3,5-triaminobenzene-2,4,6-trithiol 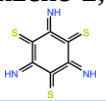	1×10^{-1} pellet	not reported	not reported	[22]
$Pd_3(BHT)$	Pd^{2+}	BHT- Benzenehexathiol	2.8×10^{-2} pellet- 4 point method	not reported	not reported	[23]
$Na_{0.9}(NBu_4)_{1.8}Fe_2(dhbq)_3$	Fe^{3+}	DHBQ- 2,5-dioxidobenzoquinone	6.2×10^{-3} pellet- 2 point method	No microporosity	N.A.	[20]
$Ni_3(HHTP)_2$	Ni^{2+}	HHTP- 2,3,6,7,10,11-hexahydroxy triphenylene 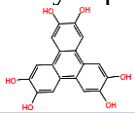	3.6×10^{-4} Sheet- 2 point method	166	not reported	[24]
$Cu[Cu(PDT)_2]$	Cu^{+}, Cu^{2+}	PDT- 2,3-pyrazinedithiolate 	10^{-4} single crystal-	not reported	0.34	[25]
$Cd_2(TTFTB)$	Cd^{2+}	TTFTB- Tetrathiafulvalene tetrabenzoate 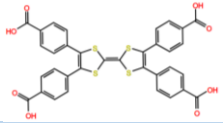	2.8×10^{-4} single crystal- 2 point method	521	0.5	[26]
$Mn_2(TTFTB)$	Mn^{2+}	TTFTB- Tetrathiafulvalene tetrabenzoate	8.6×10^{-5} single crystal- 2 point	470	not reported	[26]
$Co_2(TTFTB)$	Co^{2+}	TTFTB- Tetrathiafulvalene tetrabenzoate	1.5×10^{-5} single crystal- 2 point	531	not reported	[26]
$Zn_2(TTFTB)$	Zn^{2+}	TTFTB- Tetrathiafulvalene tetrabenzoate	4×10^{-6} single crystal- 2 point	537	not reported	[26]
NiAT	Ni^{2+}	AT- 1,3,5-triaminobenzene-2,4,6-trithiol 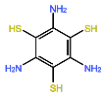	3×10^{-6} pellet	not reported	not reported	[22]

$[Sr(H_3btc)(H2O)]_n$	Sr^{2+}	H_3btc- 1,2,4-benzene tricarboxylic acid 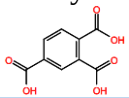	10^{-6} paste-2 point method	not reported	not reported	[27]
$Na_{0.9}[Pt_{1.5}(HTT)]$	Pt^{2+}	HTT-2,3,6,7,10,11-hexathiolatetriphenylene 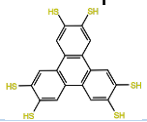	10^{-6} pellet- 2 point method	329	0.57	[28]
Fe(1,2,3-triazolate)	Fe^{2+}	1,2,3-triazole 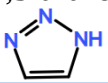	3×10^{-6} pellet-2 point method	443	not reported	[29]
$Fe_2Cl_2(BTDD)(DMF)_2$	Fe^{2+}	BTDD- bis(1H-1,2,3-triazolo[4,5-b], [4,'5'- i] dibenzo [1,4] dioxin 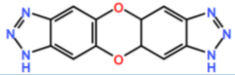	10^{-7} pellet- 2 point method	365	not reported	[29]
$Fe_2(DSBDC)(DMF)_2$ (DMF- N,N-dimethyl formamide)	Fe^{2+}	DSBDC- 2,5-disulfidobenzene-1,4-dicarboxylic acid 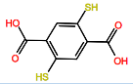	5.8×10^{-7} pellet- 2 point method	83	not reported	[29]
$Fe_2(DOBDC)(DMF)_2$	Fe^{2+}	DOBDC 2,5-dihydroxybenzene -1,4-carboxylic acid 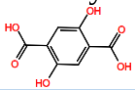	4.8×10^{-8} pellet- 2 point method	248	not reported	[29]
$Cu_3(HHTP)_2$	Cu^{2+}	HHTP- 2,3,6,7,10,11-hexahydroxy triphenylene	2.4×10^{-8} pellet- 2 point method	171	not reported	[24]
$Cu[Ni(PDT)_2]$	Cu^{+}, Ni^{2+}	PDT- 2,3-pyrazinedithiolate	10^{-8} film-2 point method	385	not reported	[30]
$Co_3(HHTP)_2$	Co^{2+}	HHTP- 2,3,6,7,10,11-hexahydroxy triphenylene	2.4×10^{-9} pellet- 2 point method	266	not reported	[24]

Interestingly, the *iridescence* of the material synthesised in this work indicated a suitable electronic structure and hence, the conductivity was measured. For metals, there is no energy band gap between the valance and conduction bands. Semiconducting materials generally have an electronic band gap less than 3.5eV with conductivity ranging from 10^{3} to 10^{-8} Scm^{-1} depending on the Fermi energy level.[31] We are not aware of any metallic conducting MOFs reported at present. Hence, characterisation of the energy band gap is significant and the phrase 'conducting MOF' will refer to a semiconducting material.[32,33]

2. Materials and methods

2.1 Selection of ligand

In the light of previous publications, the choice of ligands was based on optimising ligand to metal bonding to facilitate electron transport. This has included a wide range of metals and ligands, in some cases trying to exploit sulphur – metal interactions. However, the most effective combination is reported here where aromatic ligands have been used where there was an expectation of transport across the ligand through the π-system.

1,4-Dihydroxyanthraquinone (or Quinizarin) was also selected as it can coordinate to the metal centre through the oxygen centres of the carbonyl and hydroxyl group.

2.2 MOF preparation

MOFs were prepared via solvothermal synthesis in Teflon lined stainless steel autoclaves. The starting materials were obtained from Sigma Aldrich and used without further purification. Generally, it has proven challenging to obtain sufficiently large good quality crystals for structural determination. Indeed, very significant efforts have been made to enhance the crystal formation. However, for FeQ, very small crystals (~10um) were obtained but were large enough for single crystal X-ray diffraction via the dedicated facility available at the University of Manchester.

2.3 Characterization of materials

The materials were characterised by thermogravimetric analysis (TGA) on a TGA Q 500 at a heating rate of $10^{o}C\ min^{-1}$ under an inert atmosphere of nitrogen. Formation of a new material was evident in differences in behaviour from the starting materials. CHN quantitative analysis was done by oxidising the sample using combustion and metals and sulphur were analysed by inductively coupled plasma optical emission spectrometry measurements. BET adsorption isotherms performed on TriStar 3000 using nitrogen gas as the adsorptive at the analysis temperature of -195.8^{o}C (immersed in liquid nitrogen) were used to deduce the specific surface area.

UV-visible absorption measurements were performed to calculate the optical band gap of the materials. This was used to estimate the electronic band gap as the distinction between the two is negligible for most semiconductors. The material was finely powdered and compressed between two quartz disks for data collection on UV-Visible Varian Cary 50 Spectrophotometer 3.0. The data were collected over the wavelength range of 200-1000 nm at a scan rate of 3000 $nm\ min^{-1}$ with 0.5 nm data intervals and an average time of 0.1s in the dual beam mode. As the equipment was not set up to measure scattering, F(R) has been used analogously to absorbance

here. Due to scattering from the powder, only a range for the optical band gap could be estimated. The x-axis intercept of linear extrapolation of the Tauc plots- $(\alpha h\upsilon)^{1/2}$ versus $h\upsilon$ (direct transition) and $(\alpha h\upsilon)^2$ versus $h\upsilon$ (indirect transition) establish the end points of the optical band gap. [34,35] Here, α is the absorption coefficient (empirical), h is the Planck's constant ($6.62607004 \times 10^{-34}$ m^2kgs^{-1}) and υ is the light absoprtion frequency.

Conductivity was measured for FeQ as a pressed pellet. Four gold wire connections were made using silver doped epoxy paint. These connections were then soldered onto a puck to be used in a physical property measurement system, *DynaCool*, to measure resistance over a range of temperatures (2-400 K).

3. FeQ Synthesis

Iron(II) acetate (86.97mg, 0.5mmol) in water (5mL) is mixed into a solution of quinizarin (120.1mg, 0.5mmol) in ethanol (5mL). The mixture is heated at 175ºC for 3 days in a 23mL Teflon-lined steel autoclave and cooled slowly to 90ºC at the rate of 6ºC/hr. The mixture was kept at 90ºC for 2 days and then slowly cooled down to room temperature. The product is filtered under vacuum, washed with hot ethanol and acetone to obtain a black precipitate. Elemental Analysis: Fe-17.22, C-53.58, H-3.20; calculated for $Fe(C_{14}H_6O_4).H_2O$ Fe-17.89 C-53.88 H-2.58.

4. Results

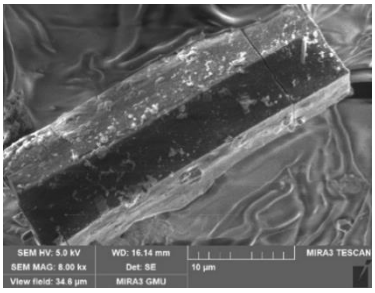

Figure 1: SEM images of FeQ shows ~10um cuboidal crystals

A black powder is obtained from the solvothermal reaction of iron(II) and quinizarin. The solvent had a significant effect on this reaction and FeQ could only be obtained in a 1:1 water-ethanol mix. The product could not be obtained in either of the pure solvents. SEM image of FeQ (figure 1) shows small crystals (~10um) which were analysed by single crystal X-ray diffraction.

X-ray crystallography shows that FeQ is a MOF that crystallizes in the space group $P2_1/c$ (details in supplementary information of deposited in the CCDC database). It has an octahedral coordination around the iron centre with each iron centre bound to three quinizarin ligand molecules as shown in Figure 2(a). Due to the asymmetry of the ligand, the phenyl groups are disordered 50% of the time at each side of the ligand but are observed to be stacking (Figure 2(b) and 2(c)) with an intermolecular distance shorter than Van der Waal's carbon radii [36], indicating π-π interaction along the organic linkers. Large elliptical channels (17Aº by 14Aº, Figure 2(d)) are also observed through the framework. Hence, it is expected that the TEA ion of size 7-7.4 A^0 (commonly used electrolyte in supercapacitors) should be accommodated.[37]

The pore width of FeQ is notable and is comparable to the largest pore width for MOFs reported to date.[38-41]

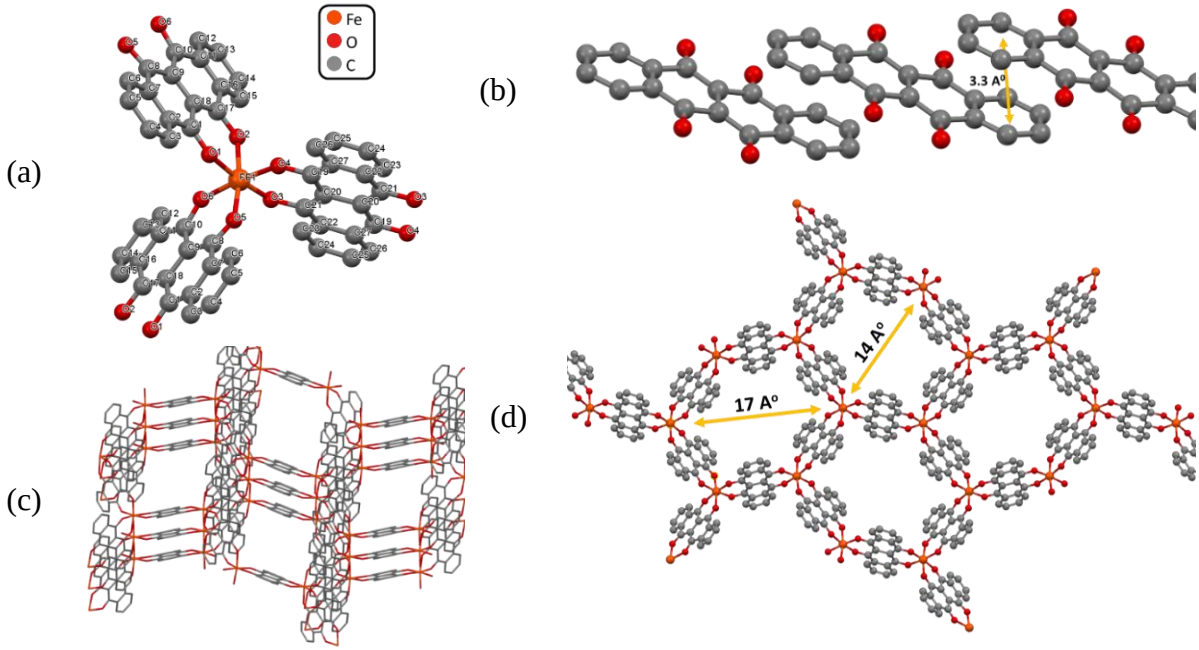

Figure 2: Crystal structure of FeQ, determined by single crystal XRD shows (a) an octahedral coordination around the iron centre with (b) a disorder in the phenyl ring of the ligand due to asymmetry and (c) a stacking of phenyl groups indicating possibility of π-π conduction. (d)View along the axis the large elliptical porous channel through the coordination framework of FeQ.

The FT-IR spectrum of FeQ (figure S2 in supporting information) supports the structure identified by the diffraction with the carbonyl stretch of the unbound ligand at 1638 cm^{-1} not observed as it is bound to the metal centre via the oxygen of the carbonyl group (table S3 in supporting information), similar to *lithiated* quinizarin, in which Li^{+} ions binds to the carbonyl oxygen of quinizarin.[42]

From the TGA data shown in Figure 3, we identify a reduction of the FeQ sample mass at approximately 270°C, suggesting it is thermally stable to up to 270°C, which is higher by 90°C than the ligand decomposition temperature (approximately 180°C). This again indicates that the ligand binding to the metal to form FeQ thermally stabilizes it.

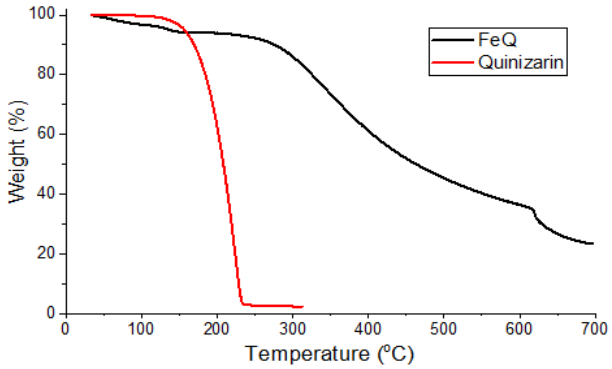

Figure 3: TGA data for FeQ. The compound (black) is stable to up to 270°C, much higher than the ligand- quinizarin (red) which decomposes at 180°C.

The specific surface area of FeQ and the activated material (solvent exchange, followed by heating *in vacuo*) were measured. It shows a porous material with a specific surface area of 29.49 m^2g^{-1} with an increase to 40 m^2g^{-1} on activation (figure S4 in the supporting information). It is markedly lower than expected from its crystal structure where 22% of the unit cell volume is expected to be solvent accessible void space and this possibly arises due to selectivity in gas adsorption, with a lower uptake for N_2. Such specificity in gas adsorption by MOFs has been reported previously.[43] This level of porosity for FeQ is similar to materials previously reported to be used for supercapacitors.[9-11]

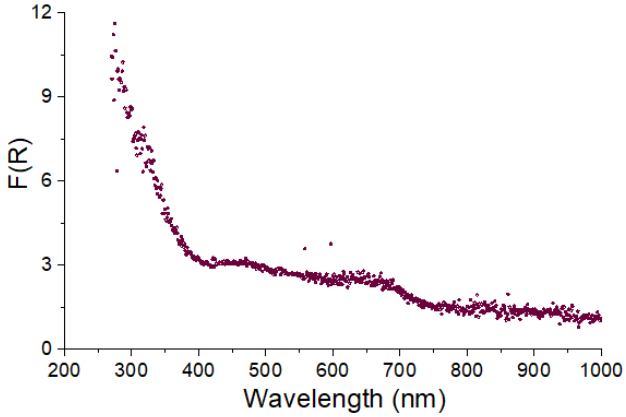

Figure 4: UV-Visible absorption spectra of F(R) against wavelength for FeQ.

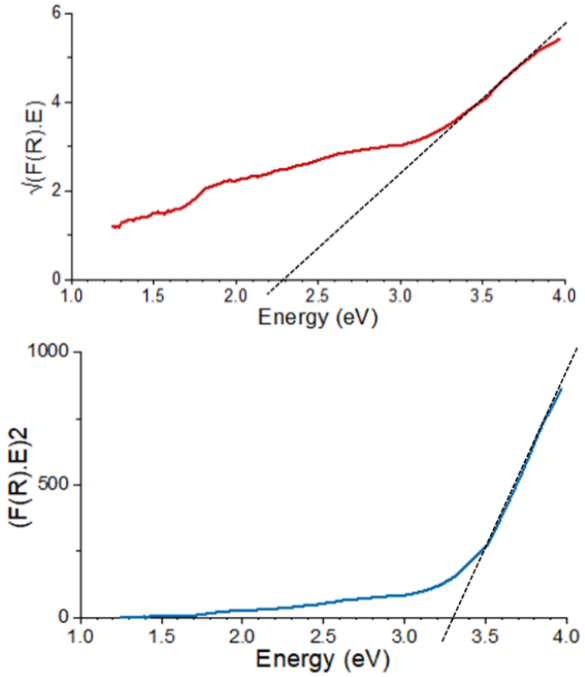

Figure 5: Tauc plots of FeQ- $(F(R).E)^{1/2}$ (direct transition, red) and $(F(R).E)^2$ (indirect transition, blue) versus energy (eV). From the linear extrapolation of absorption maxima, the estimated optical band gap range is (2.3-3.3) eV.

The band gap of FeQ was investigated using UV-Visible absorption spectroscopy as shown in figure 4. From the *Tauc* plots in figure 5, the optical band gap range is calculated to be in the range of 2.3-3.3 eV, with the absolute value dependant of the nature of transition (direct or

indirect). As the optical band gap range is below the threshold of 3.5eV, FeQ may be semiconducting. The conductivity of FeQ was measured in a pressed pellet form with the setup shown in Figure 6.

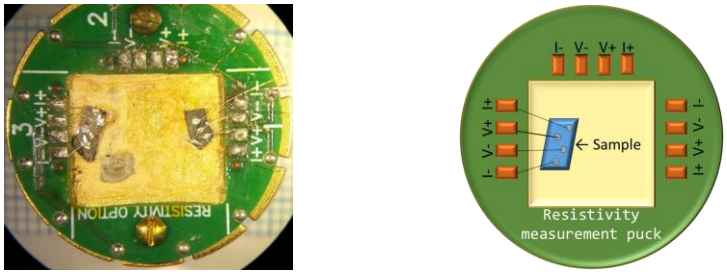

Figure 6: Image and illustration of the four-point connection setup used to measure conductivity of FeQ over a range of temperatures.

Figure 7 shows an increase in the conductivity of FeQ with temperature as characteristic of semiconducting materials. FeQ has a conductivity of 1.73×10^{-2} Scm^{-1} at 298K which increases ~three-fold on heating to 400K. Hence this material is among the highest conducting MOFs known to date. The crystal structure indicates that there is probably an anisotropic electronic conduction (along the π -stacked chains). This anisotropy will require significantly larger single crystals to facilitate measurement. However, these initial indications suggest this material may be appropriate for use in supercapacitors. The pressed pellet of FeQ can be directly further investigated as an electrode in a setup similar to *Sheberla et al*[12], which shows use of pressed pellet of $Ni_3(HITP)_2$ used as a freestanding electrode material in a supercapacitor. It has been observed that the conductivity value of a compressed pellet for anisotropic conducting material is 1-3 orders of magnitude lower due to random orientation of the material in the pellet.[44] An even higher conductivity and accessible porosity (aligned porous channels) should be attained with templated growth of this material on a substrate.

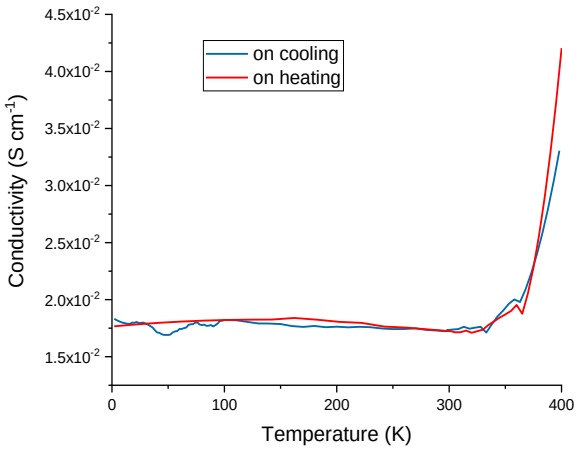

Figure 7: Conductivity of FeQ is measured to be 1.73×10^{-2} Scm^{-1} at 298K, which increases to 4.2×10^{-2} Scm^{-1} on heating the material to 400K.

5. Conclusions

In summary, the MOF formed by the combination of iron and quinizarin- FeQ has been successfully prepared. Evidence of reasonable porosity and semiconducting nature of FeQ have been presented strongly supported by single crystal diffraction. These aspects are positive indicators of useful electrode properties, possibly relevant for supercapacitors.

As far as the nature of the conduction pathways are concerned, there are several possible routes for the charge transport. In the cases of conducting MOF reported in this work, the nature of the conduction seems to be through the π-conjugation of the ligand moieties.

In terms of the challenges outlined in the introduction, the structural characteristics that a supercapacitor would have there are some positive signs. However, there is still a significant challenge to prepare deposited layers of this material on suitable substrates for ideal supercapacitor electrode.

Acknowledgements

We thank Cambridge Trust and Clare Hall for providing financial support for this work. We are grateful to Dr Matthew Cliff, Dr Andrew Flewitt, Dr Giulio Lampronti, Mr Steffen Emge, Mr Alan Dickerson, Mr Zlatko Sarasevic, Dr Changshin Jo, Dr Sian Dutton and Mr Stephen Young for assistance and guidance with the work conducted in this paper.

References

1. Burke, A. (2000). *Journal of Power Sources*, *91*(1), 37–50.
2. Kötz, R., & Carlen, M. (2000). *Electrochimica Acta*, *45*(15), 2483–2498.
3. Huang, Y., Liang, J., & Chen, Y. (2012). *Small*, *8*(12),1805-1834.
4. Zhang, L. L., Zhou, R., & Zhao, X. S. (2010). *Journal of Materials Chemistry*, *20*(29), 5983–5992.
5. Wang, Y., Shi, Z., Huang, Y., Ma, Y., Wang, C., Chen, M., & Chen, Y. (2009). *Journal of Physical Chemistry C*, *113*(30), 13103–13107.
6. Largeot, C., Portet, C., Chmiola, J., Taberna, P., Gogotsi, Y., & Simon, P. (2008). *Journal of The American Chemical Society*, *130*(9), 2730-2731.
7. Campbell, M. G., Sheberla, D., Liu, S. F., Swager, T. M., & Dincə, M. (2015). *Angewandte Chemie - International Edition*, *54*(14), 4349–4352.
8. Huang, X., Sheng, P., Tu, Z., Zhang, F., Wang, J., Geng, H., Zou, Y., Di, C., Yi, Y., Sun, Y., Xu, W. and Zhu, D. (2015). *Nature Communications*, 6(1).
9. Rajshekar Shetty, V., Gurukar, S., Marriappa, R., Kittappa, M., & Nagaraju, D. (2015). *New Journal of Chemistry*, *39*(11), 8534-8544.
10. Yang, J., Zheng, C., Xiong, P., Li, Y., & Wei, M. (2014). *J. Mater. Chem. A*, *2*(44), 19005-19010.
11. Wang, Y., Liu, Y., Wang, H., Liu, W., Li, Y., Zhang, J., Hou, H. and Yang, J. (2019). *ACS Applied Energy Materials*, 2(3), 2063-2071.
12. Sheberla, D., Bachman, J., Elias, J., Sun, C., Shao-Horn, Y., & Dincă, M. (2016). *Nature Materials*, *16*(2), 220-224.
13. Sheberla, D., Sun, L., Blood-Forsythe, M., Er, S., Wade, C., Brozek, C., Aspuru-Guzik, A. and Dincă, M. (2014). *Journal of the American Chemical Society*, 136(25), 8859-8862.
14. Kobayashi, Y., Jacobs, B., Allendorf, M. D., & Long, J. R. (2010). *Chemistry of Materials*, *22*(14), 4120–4122.
15. Talin, A., Centrone, A., Ford, A., Foster, M., Stavila, V., Haney, P., Kinney, R., Szalai, V., El Gabaly, F., Yoon, H., Léonard, F. and Allendorf, M. (2013). *Science*, 343(6166), 66-69.
16. Low, K.-H., Roy, V. A. L., Chui, S. S.-Y., Chan, S. L.-F., & Che, C.-M. (2010). *Chemical Communications*, *46*(39), 7328.
17. Dou, J., Sun, L., Ge, Y., Li, W., Hendon, C., Li, J., Gul, S., Yano, J., Stach, E. and Dincă, M. (2017). *Journal of the American Chemical Society*, 139(39), 13608-13611.
18. Campbell, M. G., Sheberla, D., Liu, S. F., Swager, T. M., & Dincə, M. (2015). *Angewandte Chemie - International Edition*, *54*(14), 4349–4352.

19. Jia, H., Yao, Y., Zhao, J., Gao, Y., Luo, Z., & Du, P. (2018). *Journal of Materials Chemistry A, 6*(3), 1188-1195.
20. Darago, L. E., Aubrey, M. L., Yu, C. J., Gonzalez, M. I., & Long, J. R. (2015). *Journal of the American Chemical Society, 137*(50), 15703–15711.
21. Kambe, T., Sakamoto, R., Hoshiko, K., Takada, K., Miyachi, M., Ryu, J., Sasaki, S., Kim, J., Nakazato, K., Takata, M. and Nishihara, H. (2013). *Journal of the American Chemical Society*, 135(7), 2462-2465.
22. Sun, X., Wu, K., Sakamoto, R., Kusamoto, T., Maeda, H., Ni, X., Jiang, W., Liu, F., Sasaki, S., Masunaga, H. and Nishihara, H. (2017). *Chemical Science*, 8(12), 8078-8085.
23. Pal, T., Kambe, T., Kusamoto, T., Foo, M., Matsuoka, R., Sakamoto, R., & Nishihara, H. (2015). *Chempluschem*, *80*(8), 1255-1258.
24. Mendecki, L., Ko, M., Zhang, X., Meng, Z., & Mirica, K. (2017). *Journal of The American Chemical Society*, *139*(48), 17229-17232.
25. Takaishi, S., Hosoda, M., Kajiwara, T., Miyasaka, H., Yamashita, M., Nakanishi, Y., Kitagawa, Y., Yamaguchi, K., Kobayashi, A. and Kitagawa, H. (2009). *Inorganic Chemistry*, 48(19), 9048-9050.
26. Park, S., Hontz, E., Sun, L., Hendon, C., Walsh, A., Van Voorhis, T., & Dincă, M. (2015). *Journal of The American Chemical Society*, *137*(5), 1774-1777.
27. Usman, M., Mendiratta, S., Batjargal, S., Haider, G., Hayashi, M., Rao Gade, N., Chen, J., Chen, Y. and Lu, K. (2015). *ACS Applied Materials & Interfaces*, 7(41), 22767-22774.
28. Cui, J., & Xu, Z. (2014). *Chem. Commun.*, *50*(30), 3986–3988.
29. Sun, L., Hendon, C., Park, S., Tulchinsky, Y., Wan, R., Wang, F., Walsh, A. and Dincă, M. (2017). *Chemical Science*, 8(6), 4450-4457.
30. Kobayashi, Y., Jacobs, B., Allendorf, M. D., & Long, J. R. (2010). *Chemistry of Materials*, *22*(14), 4120–4122.
31. Kulphaldt, T.R. *Lessons in Electric Circuits- Volume III Semiconductors*. All About Circuits, 2009.
32. Usman, M., Mendiratta, S., & Lu, K. (2016). *Advanced Materials*, *29*(6), 1605071.
33. Alvaro, M., Carbonell, E., Ferrer, B., Llabrés i Xamena, F., & Garcia, H. (2007 *Chemistry - A European Journal*, *13*(18), 5106-5112.
34. Hong, S. J., Lee, S., Jang, J. S., & Lee, J. S. (2011). *Energy & Environmental Science*, *4*(5), 1781.
35. Zhang, G., Lan, Z.-A., Lin, L., Lin, S., & Wang, X. (2016). *Chemical Science*, *7*(5), 3062–3066.
36. Bondi, A. (1964). *The Journal of Physical Chemistry*, *68*(3), 441-451.
37. Ikuno, T., Chaikittisilp, W., Liu, Z., Iida, T., Yanaba, Y., Yoshikawa, T., Kohara, S., Wakihara, T. and Okubo, T. (2015). *Journal of the American Chemical Society*, 137(45), 14533-14544.
38. Eddaoudi, M., Kim, J., Rosi, N., Vodak, D., Wachter, J., O'Keeffe, M., & Yaghi, O. (2002). *Science*, *295*(5554), 469-472.
39. Li, H., Eddaoudi, M., O'Keeffe, M., & Yaghi, O. (1999). *Nature*, *402*(6759), 276-279.
40. Stephen S.-Y. Chui, Samuel M.-F. Lo, Jonathan P. H. Charmant, Orpen, A., & Williams, I. (1999). *Science*, *283*(5405), 1148-1150.
41. Guillerm, V., Xu, H., Albalad, J., Imaz, I., & Maspoch, D. (2018). *Journal of The American Chemical Society*, *140*(44), 15022-15030.
42. Yang, J., Xiong, P., Zheng, C., Qiu, H., & Wei, M. (2014). *J. Mater. Chem. A*, *2*(39), 16640-16644.
43. Humphrey, S. M., Chang, J. S., Jhung, S. H., Yoon, J. W., & Wood, P. T. (2007). *Angewandte Chemie-International Edition*, *46(1–2)*, 272–275.
44. Wudl, F., & Bryce, M. R. (1990). *Journal of Chemical Education*, *67*(8), 717.